Optional cause to Alzheimer disease: too high screening of the electromagnetic mutual-inductance between axons in the brain

Israel Fried*

*Space physicist (M.Sc.), Independent theoretical researcher in physics and biology
http://ifried22.tripod.com
ifried22@gmail.com

Abstract

Electromagnetic (EM) **self**-inductance of a single axon about itself was measured and show no significant influence on the electric conductance in the axon (Scott 1971). Recent works regard EM **mutual inductance** (EMMI) between **parts of the same axon**. AS far as I know, there is no work regarding EMMI between **different** axons. Here suggested a theoretical option that too high screening of EMMI between **many** axons in the brain causes to the Alzheimer disease (AD). Accordingly, suggested **theoretical** options for preventing AD and using EEG for monitoring EMMI shielding, and thus, AD status. Also, suggested research methods for proving EEMI between multi myelinated axons and its screening. Also suggested to measure the memory of many million people during a major geomagnetic storm on Earth due to sun eruption, in order to find out the level of shielding in many million people and getting alarm, years before the common signs of AD appears, and start active actions to prevent AD.

Note: Since the ideas in this article are theoretical, yet without laboratory research, one should not regard these ideas as clinical suggestions.

1. **Introduction**

As well known, in myelinated axons exists alternate electric current due to the saltatory conductance between the Ranvier nodes. The physical equations of electrical conductance in axons described in (Opatowski 1950). The saltatory conductance described in the model of (Hodgkin and Huxley 1952) which base on the physical equations of alternate electric current. The myelin and their Ranvier nodes enable increasing by a factor the conduction velocity of sodium ions inside the axon, compared to bar-axon. The opening and closing of ion channels in Ranvier node enable insert of Na^+ and exit K^-. Hence, the electric sign, at the edge of the Ranvier node, alternates from negative rest voltage, say -30 mV, to positive active action, say +70 mV. The myelin insulates the surrounding from the inside electric currents, but not from the magnetic fields that created due to the motion of electricity within the axon. The strength of the magnetic field depends, among other factors, on the internal velocity of the electrical current. Hence, alternating electric current inside the axon creates alternating magnetic field in the axon's surrounding. This creates, in return, weaker electric current in the opposite direction (Lenz law) inside the same axon (self-inductance) or inside other axons (mutual-inductance). Scot show mathematically that the **self**-inductance over a large axon of octopus is *negligible by five magnitude orders* relative to a significant influence (Scot 1971). The magnetic field about a *single* nerve was first measured by (Roth and Wiksow 1985). Nowadays, such measurements used in clinic, see e.g. (Wijesinghe 2010). In addition, there are works for inducing electric currents within axons in the brain, using *external* magnetic field, see e.g. (Rotem and Moses 2008). Recent works regard EM *mutual*-inductance (EMMI) between axons and their schwann cell myelin-protein sheaths (Goodman and Bercovich 2013), as well as between the adjacent myelin sheaths of the same axon (Wang et al 2018).

Here discussed, for the first time as far as I know, a theoretical option for EMMI between *different* axons in the brain. As shown in the following, EMMI between *two* axons has influence on their electric conductance much less than in self-inductance. However, EMMI between a single axon and between many other axons might be significant, regarding the electric conductance of that single axon. In the brain are structures of multiple *parallel* myelinated axons. We shall mainly treat those in the corpus callosum (CC), which used for communications between the two hemispheres. The EMMI might influence those communications and responsible to various normal brain functions. In addition, as in any electromagnetic system, there is a *normal* EMMI *screening* between those many axons in the brain. Too high or too low screening might affect the normal brain functions. Here we discuss a theoretical option that too high screening of EMMI might lead to the Alzheimer disease (AD).

Sec. 2 discussed the methods for mutual inductance between parallel axons, including basic physics of EMMI; characteristics of parallel myelinated axons; EMMI between **two** parallel axons, and EMMI between axon-2 and parallel many others. In Sec. 3 shown theoretical results of EMMI for many parallel axons. Sec. 4 discussed those results. In Sec.5 suggested optional influences of EMMI on brain functions, especially on transverse communications (TC), which is differs than the known longitudinal communications (LC) via the synapses. Sec. 6 discussed optional screening of EMMI in the brain and Sec. 7 discussed optional reasons to creation of too high screening. Sec. 8 suggested to use EEG for monitoring AD status. Sec. 9 suggests **a** research for proving EEMI between multi myelinated axons and its screening. In Sec 10 suggest to measure the shielding, s_{bmi}, in the brains of many million people during Sun Eruptions, in order to find out the level of shielding in many million people and getting alarm, years before the common signs of AD appears, and start active actions to prevent AD. In SA given a model of axons at many concentrating circles. At the end giving the meanings of short terms in this article.

Note: Since the ideas in this article are theoretical, yet without laboratory research, one should not regard these ideas as clinical suggestions.

2. Mutual inductance between parallel axons - Methods

In this Sec. 2 discussed a theoretical model of mutual inductance between parallel axons. We start with basics physics regarding **e**lectromagnetic mutual induction (EMMI) phenomenon. Than we treat the parameters of parallel myelinated axons in human brain. In Sec. 2.3 developed the theory for EMMI between two parallel axons. Than we use these principles for evaluating EMMI of many parallel axons that pass via the CC.

2.1. Basic physics of electromagnetic mutual inductance

EMMI is the phenomenon where a changing electric current in a conductor creates a changing electrical current in another conductor although there is no direct contact between the two conductors. As in electric cables, the electrical current, I, of a conductor of length l, creates at its surrounding a magnetic field, B, which its value at distance $d << l$, vertical to the conductor, is

$$B = \mu \frac{2I}{d}, \tag{1}$$

while μ is the magnetic permeability of the medium surrounding the conductor. In free space $\mu_0 = 4\pi x10^{-7}\ hm^{-1}$, which is very close to that of air. We shall see later that the value of μ in the brain is close to that of μ_0. In addition, for strong magnetic fields the value of μ depends on the magnetic field, B. However, within the axons in the brain, the electric threshold currents are very weak, magnitude order hundreds pA, see e.g. (Grubb and Burrone 2010), compared to several amperes (A) in electric wires for home transformer. Hence the magnetic fields in the nervous systems are very weak, which means μ is independent on the internal magnetic fields due to currents within the axons.

Let us regard two straight parallel conductors, with small circular cut surfaces, at distance *d*, and let conductor-1 has current I_1. A magnetic flux, ϕ, created in the surrounding of conductor-1 passes via conductor-2 as well. Let the cut surface of conductor-2 be A_2 and let B_2 be the magnetic strength within this cut. Since the cut surface is small, we regard B_2 as constant. Hence, the magnetic flux within conductor-2, due to the current in conductor-1 is

$$\phi_{21} = B_2 A_2 = \mu \frac{2I_1}{d} A_2 . \tag{2}$$

With the relative position of the two conductors fixed, ϕ_{21} is proportional to I_1. Upon changing I_1 with time, electromotive force (emf) created in conductor-2

$$\varepsilon_{21} = -M_{21} \frac{dI_1}{dt}, \tag{3}$$

where the coefficient M_{21} is the **mutual inductance** in conductor-2 due to current in conductor-1. The units of ε and *M* in SI are v and h, respectively. *M* depends on the geometry of the conductors as well as on the magnetic permeability μ. The minus sign is due to Lenz's law. We shall see later the importance of this minus sign to the start of AD. Now, let us connect the two ends of conductor-2 to a resistant, and let the impedance be Z_2. Due to Ohm's law, the alternating current in conductor-2 is

$$I_2 = \frac{\varepsilon_{21}}{Z_2} . \tag{4}$$

Thus, upon giving the geometry of the conductors, the value of μ and the rate of change of the current in conductor-1, one may obtain the changing current in conductor-2, although the two conductors have no direct contact. This is the meaning of electromagnetic mutual induction.

2.2. Parallel myelinated axons

In this sub-Sec. discussed the parameters of parallel myelinated axons. We know that in the nervous system there are many cases of parallel axons, which include curled up axons. In addition, the axons have mainly elliptical cut surface shapes which are close to circles. There is an essential difference between the electric conduction in axons and that of electric wires. In parallel axons, the electric conduction is due to chemical rates at the synapses and due to mutual inductance between the axons, which influences the conducting rate and the chemical rates, while in electric wires the mutual inductance not influence the voltage rate of the generator. Regard two parallel axons having initial currents at the exits from their own body–nerves. During the travel to synopses, the mutual inductance

might change their current strength. In electric cable lines those changes might be regarded as losses of electrical energy. Engineers search ways to decrease this mutual inductance by shielding the cables using plastic or other diamagnetic covers. On the other hand, in the brain those changes might be the key to understanding its various functions.

We discuss here mainly the parallel axons in the CC. Most of them are myelinated axons. The myelin layer insulates the surrounding from the electricity within the bare axon. However, it does not insulate the magnetic field. The myelin thickness depends on the number of myelin sheets about the bare axon. In many cases the myelin thickness is 1/3 the internal axon radius. Another important point is the great density of myelinated axons in the human CC. Its area is 5 – 7 cm^2 , see Table A2 in (Bishop and Wahlsten 1997). According to (Collin et al 2016) the CC contains about 200 – 250 million axons that cross the CC for connecting the two hemispheres. Hence the density of the parallel axons greater than 285,000 axons/mm^2.

In Fig. 4 of (Liewald et al 2014) shown the way they measured the inner diameter of myelinated axons. Most of the axons have *elliptical* shape. The measured diameter, D_{inner}, is the *short* axis of the ellipse. In addition, as shown in Fig. 7 of (Liewald et al 2014), the axons in a small section of the CC of a monkey Macaque have various diameters. This is also true for human CC. Thus, if one wishes to compute the mutual inductance between a specific axon and between all the other axons, one should regard the various diameters and distances of the axons in that section. However, as in many cases in electrodynamics, since the conduction velocity increases approximately linearly with axon diameter (Hursh 1939), one may use equivalent method: Regard a specific section with myelinated axons of various internal diameters. Let the *mean* internal diameter of the axons be D_{mean} and let the section area be $A_{section.}$. This is the cut surface that includes the axons, each of which is a cut surface of a myelinated axon, as in the case of the splenium. In Supplementary A (SA) shown how to get the circular inner radius, R_{inner}, for a circle of the same area as that of the inner ellipse of the bar-axon, without myelin. We shall use this inner radius for computing the EMMI between *two* axons.

2.3. EM mutual inductance between two parallel axons

The task now is to evaluate M_{21} for two parallel axons of the same length. Since we deal in this paper with the EMMI of axons, and since they have radii in the order of 1 μm, we may use the formulae given in (Aebischer and Aebischer 2014) for very small wires, magnitude orders mm, which used in the microchips technology. In Eqs. 62 and 63 of that paper given the formula for the EMMI between two *straight parallel* conductors, at air medium, made up of non-magnetic material, with *circular* cut of the same radius and the same length. Using that formula in our case of two parallel axons in CC leads to

$$M_{21,\,axons} = \frac{\mu_{inter-nerves}}{2\pi}\left[l_{axon}\cdot\ln(G+l_{axon}) - l_{axon}\cdot\ln d_{two\,axons} - G + d_{two\,axons} + \frac{R_{inner}^2}{4d_{two\,axons}}\right], \quad (5)$$

where

$$G \equiv \sqrt{l_{axon}^2 + d_{two\,axons}^2 + R_{inner}^2}\,, \quad (6)$$

and $M_{21,\,axons}$ is the EMMI over axon-2 due to alternate current in axon-1; R_{inner} is the radius of their circular cut, which is the same for both, following conversion from elliptical axon to circular shape, as shown in (S1) - (S3) of SA ; $d_{two\,axons}$ is the distance between the two axons, which includes the myelin thickness and the space between the myelinated axons ; l_{axon} is the length of the axons, which assumed by the model to be the same for all the parallel axons; and $\mu_{\text{inter}-nerves}$ is the magnetic permeability of the matter between those two axons.

One may regard the axon section that drawn from the exit point in the body-nerve to the end point at the first synapse, as a closed electric loop. In both cases, electric quantities exit from one point and spill into another point. This transfer of electrical quantity from one point to another may be regarded as due to electromotive force (emf). The emf created in axon-2 due to change of current in axon-1, see (3), is

$$\varepsilon_{21,\,axons} = -M_{21,\,axons}\frac{dI_{1,\,axon}}{dt}. \tag{7}$$

Regard the gradient of current with time, dI_{axon}/dt. As mentioned in (Liewald et al 2014), for internal axon diameter greeter than 0.6 micron of myelinated axons, the conduction velocity increases approximately linearly with axon diameter. Since we do not know the connection between axon diameter and conduction velocity for axons with diameter less or equal 0.6 micron, we apply, for our representation, that linear connection for all diameters, say down to 0.1 micron. Since the dependence of the conduction velocity on time is like the dependence of the current on time, see (Scott 1971), it is reasonable that the dI_{axon}/dt increases approximately linearly with axon diameter. Hence, upon giving dI_{axon}/dt for axon-1, one may obtain the parallel for axon-2 by

$$\frac{dI_2}{dt} = \frac{dI_1}{dt}\frac{D_1}{D_2}. \tag{8}$$

Use this equation for various axon's diameters and insert the result into (7) yields the emf created in axon-2 due to change of current in axon-1.

2.4. EM mutual inductance between axon-2 and many others

In this sub-Sec. we use the equations of sub-Sec. 2.3 for developing the theory of EMMI between axon-2 and between many others parallel to axon-2. From Fig. 7 of (Liewald et al 2014) there is about a constant space between the myelinated axons, regardless the axon diameter. This space required for the saltatory conduction mechanism, i.e. to supply the Na^+ from the surrounding of the Ranvier node. In SA we also show how to get the following: a) the radius of a circular myelinated axon, $R_{myelin-axon}$, that includes the myelin width. b) the radius of a *tiny* circle about the axon, $R_{tiny} \equiv R_{myein-axon} + \delta_{space}$, where $2\delta_{space}$ is the distance between the myelin surfaces of two nearby myelinated axons. In the following we shall see that δ_{space} is one of the most important parameter for determining the optional

screening of EMMI between axons, which we regard here as important for understanding the Alzheimer disease. c) Building the theoretical model of many tiny circles in circular layers about axon-2 at the system origin, without space between the layers so that the first layer has 6 tiny circles; the second layer 12, and so on i.e. increasing by 6 from one layer to the next. Using this model to compute the number of tiny circles, N_{tiny}, in given area of the cut surface at the center of the splenium, and computing the maximal number of layers, $n_{\max}$, in that system. Now, using (5), the total mutual inductance over axon-2 is

$$M_{2,(N_{tiny}-1)} = \sum_{n=1}^{n_{\max}} M_{21,n} \,. \tag{9}$$

We use the Excel programming for exact computation of (9), while $n_{\max}$ is of orders $10^3 - 10^4$. In our case of the same diameters for all the $(N_{tiny}-1)$ axons, we may write

$$\frac{dI_{(N_{tiny}-1)}}{dt} = (N_{tiny}-1)\frac{dI_{1,\,axon}}{dt} \,. \tag{10}$$

Hence, the parallel to (3) is now

$$\varepsilon_{2,(N_{tiny}-1)} = -M_{2,(N_{tiny}-1)} \frac{dI_{(N_{tiny}-1)}}{dt} \,. \tag{11}$$

In the following shown that although $\varepsilon_{21axons}$ is too small to be significant, the case of large enough N_{tiny} leads to a significant value of emf in axon-2.

3. Results for many parallel axons

3.1. Input data

In this Sec. we use the above equations for evaluating the emf in axon-2 for two cases: a) two parallel axons. b) many parallel axons. Let us use (5) for two parallel axons in the splenium of an adult human CC. The CC is a part of the cortex, is the largest white part in the brain since it mostly contains myelinated-axons. Many of the thin axons in CC, of diameter less than 1.0 μm, appear in the splenium. In Table 4 of (Abiotiz et al 1992) given the mean area of the splenium of adult males as $A_{splenium} = (170 \pm 26)\, mm^2$. In Table 1 of (Liewald et al 2014) given the measured mean and SD values for internal diameters in a small area of the splenium as $D_{splenium} = (0.70 \pm 0.56)\, \mu m$. For the representation here we adopt this mean and SD values for the entire splenium area. Since the axons pass via CC in two directions, between the two hemispheres, and since we wish to work here with axons that their conductive velocities are parallel and advance along the same direction, we divide the area by 2, i.e. $A_{\sec sion} = (8.5 \pm 0.13)\text{x}10^{-5}\, m^2$. From Fig. 7 of (Liewald et al 2014), the minimal distance

between two nearby myelin membrane seems, after enlarging that Fig 7 by 1600, as less than $4x10^{-8}$ m. To be on the safe side we take for our representation $\delta_{space} = 5x10^{-8}\ m$.

For applying (5) we also need a value for l_{axon}, i.e. the axon length. From Table 2 of (Caminiti et al 2013) we see that the mean length of axons from their source point to the midline of the human CC, at the splenium, i.e. temporal plus visual in the notation of that paper, is $(75.20 \pm 4.88)\ mm$. Since in our model we seek for the axon length from its source to its target nerves, we multiply this value by 2, and disregard the error, i.e. $l_{axon} = 0.1504\ m$. In addition, since $\mu_{\text{inter-nerves}}$ is very close to μ_0, as we shall see later, and does not essentially influence our computational results, we use here $\mu_{\text{inter-nerves}} = \mu_0$.

Now, we wish to use (3) for gross evaluation of the emf induced in axon-2 at the human splenium due to changing current in a parallel nearby axon-1. As far as I know, there is yet no data regarding the currents' amplitudes and rates of axons in the brain. Hence, for gross evaluations I shall use known data regarding other axons. There are various types of axons. Generally, the action potential is - 70 mV to +30 mV which advances in velocities 0.5 - 120 m/s. The action potential in axon changes on a scale time of a few ms.

From Table S2 of (Caminiti et al 2009) we see that the conduction velocity in m/s of action potential is approximately proportional to the internal diameter, for 1 - 1.4 μm, of myelinated axons in Human CC. The ratio is $(7.84 \pm 1.34)\ ms^{-1} / \mu m$. Hence, the current in axon changes in scale of ms as well. From Fig. 3(b) of (Bakiri et al 2011) there is a difference of 483 pA in electric current of the membrane of oligodendrocytes (the cells that create the myelin sheath over the axons) in the CC, during 200 ms, i.e. $dI_{olig} / dt = 2.4x10^{-9}\ A/s$. AS far as I know, this is the only record for dI/dt in human brain. However, the membrane of oligodendrocytes has different function than the membrane of the thinnest axon in the splenium. The last one should transfer currents in much greater velocity and rate, optionally greater by several magnitude orders. From Fig. 10(b) of (Liewald et al 2014) we see that the smaller internal axon diameter in the splenium of human brain 3, is 0.2 micron. Thus, as a representative value for dI/dt of human splenium axon, with internal diameter 0.2 micron, we multiply by 10 only the value of the oligodendrocytes membrane, i.e.

$$\frac{dI_{D=0.2}}{dt} = 2.4x10^{-8}\ A/s\,. \tag{12}$$

Using this value, one may apply (8) to obtain dI/dt for axons with various internal diameters.

3.2. Output results

Now, we are ready to apply the above set of equations, including those in SA, to obtain the emf induces to a single axon, within the human splenium, by the EEMI with the entire other axons in the splenium. In Table S1 of SB given the input data and output results for cases where the entire human splenium contains many of the same myelinated axons, with mean internal diameters 0.1 – 1.0 micron.

In Table 1 given the two rows from Table S1 regarding $\varepsilon_{2,1}(10^{-17}mV)$ and $\varepsilon_{2,N}(mV)$ vs $D\,(10^{-7}\ m)$. In Fig. 1 given the histograms of those two rows. The value of *N* is the value of $(N_{tiny}-1)$ in Table S1 for each internal diameter.

Table 1. The emf between axon-2 and 1 or N axons, multiplied by (-1), vs the axon diameter. Notice the scales of the two first columns. The last column shows $\varepsilon_{2,N}$ is significant, compared to +30 mV of axonal conductive potential.

D	-e2,1	-e2,N	e2,N/30
(E-7 m)	(E-17 mV)	(mV)	(%)
1	0.565	1.510713	5.04
2	1.083	0.402552	1.34
3	1.580	0.159064	0.53
4	2.061	0.07813	0.26
5	2.531	0.043946	0.15
6	2.992	0.027118	0.09
7	3.445	0.017888	0.06
8	3.892	0.012407	0.04
9	4.334	0.008962	0.03
10	4.770	0.006679	0.02

Fig. 1. A: emf in axon-2 of internal diameters 0.1 – 1.0 micron, due to EMMI with the other axons in the splenium with the same internal diameters 0.1 – 1.0 micron, respectively. B: emf in axon-2 of internal diameters 0.1 – 1.0 micron, due to EMMI with a *single* nearby axon, in the splenium, with the same diameter.

A

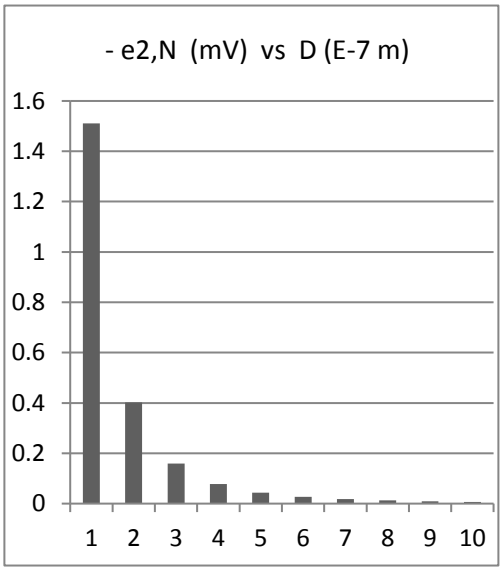

B

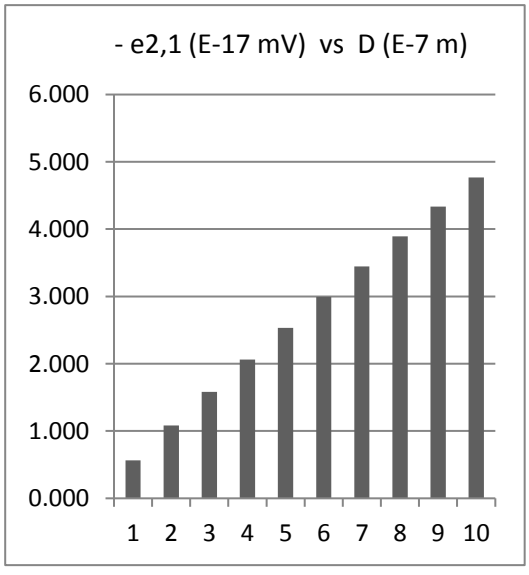

4. Discussing the results

The results obtained in Sec. 3 are very interesting. We see from Table 1 and Fig. 1 that the absolute value of $\mathcal{E}_{2,N}$ decreases while D increase. On the other hand, the value of $\mathcal{E}_{2,1}$ increases with D. The values of $\mathcal{E}_{2,1}$ are clearly far from being significant, upon considering the myelinated axonal conductive potential -70 to + 30 mV. However, the values of $\mathcal{E}_{2,N}$ are *significant*, compared to the conduction potential of those axons. In the last column of Table 1 given the ratios (in %) between the absolute value of $\mathcal{E}_{2,N}$ and the 30 mV of the axonal conductive potential. The range is from 5% for D = 0.1 micron through 0.02% for D = 1.0 micron. These are significant ratios that might be very important for the brain functions, as shown in the following.

Regard the minus signs in the second column of Table 1. That means the multi-mutual inductance leads to a small change in the main conductive potential of axon-2. Since axon-2 is taken here for the mathematical model, this small change might occur in any axon of the large group of axons. The change might be a small reduction in amplitude, or a small change of the frequency of the main conduction potential, etc. Hence one may regard the small emf, due to multi-mutual inductance, as a kind of a *"signal input"* into a "carrier wave", which is the alternating conduction potential via the synapses. In telecommunications, the "signal input" may be transmitted by modulation of the carrier wave. There are various ways of modulations, e.g. amplitude modulation (AM), frequency modulation (FM), phase modulation (PM), etc. Hence, here suggested the option there are two kinds of communications in the brain. a) longitudinal communication (LC) via the synapses at the terminals of the axons. b) transverse communications (TC) via parallel input signals due to EM multi-axonal inductances between axons. The TC might yield the familiar EEG waves, since one may see in EEG waves various kinds of modulations. Also, suggested to search whether the transverse waves use for brain's mental functions. The multi-mutual inductances by many axons enable, in addition, various super-positions. Hence, all we know from technological communications might exist in the brain, due to those significant emf, due to multi-mutual inductance. Moreover, some of the neurological disease might be due to disturbance to the multi-mutual inductance. In the following shown the option that AD might be due to such disturbance.

5. Optional influences of mutual inductions on brain functions

We saw that between large numbers of axons there might be significant EMMI. This raises the theoretical option that brain functions are due to internal communications, by EMMI, between *groups* of nerves, rather than between single nerves. Let us call such optional phenomenon "axons groups mutual inductance" (AGMI). This option might explain why we remember in terms of entire events rather than in terms of single bits as a computer does. For example, when our eyes see a picture, the brain does not treat single retinal sensors but complete pictures that might lead us to remember a complete audio event by using AGMI. Even if our finger stubbed by a tiny pin, there might be involved AGMI in the reflex. Our memory, thoughts, learning, motor-sensors loops, and many more brain functions might be due to AGMI. The main advantage of AGMI is there is no necessary for direct connection between the axon's groups via synapses. Hence communication by AGMI is much faster and enables immediate response to critical situations. The mechanism of EMMI enables repeated influences between the electrical conductions of two untouched axons. A simple option is sinusoidal fluctuations of electric currents in the axons, in addition to the alternate current due to the biological mechanism in axon. Such sinusoidal fluctuations might be the key for keeping data. When considering AGMI there

might be *resonances* of electrical conductions in many axons. This might lead to a memory by association.

6. Screening of EM mutual inductance in the brain

Now that we saw the optional importance of EMMI on brain functions, including TC , we wish to learn the options for disturbing those functions. It is known that within the brain of patients with AD found high amounts of the biological materials β-Amyloid plaques and Tau tangles. βA are peptides without iron in their compounds. Hence, according to e.g. (Schenck 2000) they are diamagnetic, i.e. with negative susceptibility. Notice that recent work (Plascencia-Villa et-al 2016) shows that *within* the **core** of a big spherical βA there are accumulations of iron oxide (Fe_3O_4) magnetite nanoparticles that perform nanostructured particles in channels of diameter 8 μm within the core of βA. Hence, the big spherical βA is diamagnetic with respect to an outside observer, although its center contains super-paramagnetic nanoparticles. Thus, the envelope of βA screens the environment from the super-paramagnetic core. In addition, it increases the screening of the mutual inductance between axons in the brain. Hence, accumulation of many big spheres of βA plaques decreases the magnetic susceptibility of the inter-nerve medium bellow its normal low limit, $\mu_{\text{int}\, nervs-low}$, which means increasing the screening of EMMI between axons in the brain. Regarding the Tau tangles proteins, there is no evidence they include iron. Thus, they are diamagnetic, as most biological materials. Tau tangles created in the brain, mainly due to destruction of axons.

I recognize (theoretically) two main mechanisms for creating too high EMMI screening: a) the accumulation of βA plaques in the inter-nerve medium, between two specific axons, leads to decreasing of the EMMI between those two axons. Thus, their normal functions reduced. In extreme accumulation of βA plaques, the two specified axons destructed. b) Destruction of axons leads to accumulation of Tau tangles. This decreases the susceptibility of the inter-nerve medium between two *other* axons in the vicinity to those two specific axons. Thus, the screening between the two other axons increases, and the process, of functions reduction in axons as well as their destruction, repeats itself. Hence, we define here two critical levels of M_{21}: the preventing level, $M_{21-prevent}$, and the destructive level $M_{21-destruct}$, so that

$$M_{21-destruct} < M_{21-prevent} < M_{21-normal-low}. \tag{13}$$

For obtaining the critical values of M_{21}, one needs the values of the magnetic permeability in the various cases.

Due to using strong magnet fields in modern facilities, such as MRI, fMRi, etc. it is important to reveal the magnetic characteristics of biological materials. Materials that repulse magnetic flux are known as diamagnetic. They have magnetic permeability less than that of vacuum, $\mu < \mu_0$. Another way to express this inequality is to say the susceptibility, χ, of those materials is negative, where susceptibility defined by the connection $\mu = \mu_0(1+\chi)$. Notice, the parameter χ is dimensionless. Positive χ means ferromagnetic or paramagnetic matter. The importance of using χ is mainly for cases of relative tiny values. In the literature are tables of susceptibilities for various compounds. According to (Schenck 2000) the susceptibility of most human tissues are in the range -7.0 to -11.0 ppm. Regard ferromagnetic

material such as iron. For adult human of 70 kg weight the total amount of iron is 3.5 g. Here is an important citation from (Schenck 2000) regarding iron compounds: "they are distributed in various chemical compounds, such as hemoglobin, ferritin and hemosiderin, which are only weakly paramagnetic and do not interact strongly with applied fields. **The concentrations of these paramagnetic substances are not large enough to convert the overall susceptibility of any tissue (including blood) from diamagnetic to paramagnetic"**. In (Zborowski et al 2003) the magnetic susceptibility (in SI units) of water is $\chi_{H_2O} = -9.035x10^{-6}$; for fully oxygenated red blood cell $\chi_{RBC_{oxy}} = -9.249x10^{-6}$, i.e. *lower* than water; for fully deoxygenated red blood cell $\chi_{RBC_{deoxy}} = -5.705x10^{-6}$, i.e. higher than water. Using these data, let us regard a parameter $\chi_{\text{int}nervs}$ so that $-9.249x10^{-6} \le \chi_{\text{int}nervs} \le -5.705x10^{-6}$. Now, we may write $\mu_{\text{int}nervs} = \mu_0(1+\chi_{\text{int}nervs})$. Hence, the upper and lower *normal* limits of $\mu_{\text{int}nervs}$ are

$$\mu_{\text{int}nervs-upper} = \mu_0(1-5.705x10^{-6}); \qquad \mu_{\text{int}nervs-lower} = \mu_0(1-9.249x10^{-6}) \quad . \tag{14}$$

The $\mu_{\text{int}nervs-lower}$ may be used to calculate the $M_{21-normal-low}$ that limits the critical EMMI in (13).

The maximal number of beta Amyloid, βA, sheathes in the space between two parallel axons, δ_{space}, is

$$N_{\beta A-\max} = \frac{\delta_{space}}{W_{\beta A}}, \tag{15}$$

where $W_{\beta A}$ is the width of a single ribbon of βA. According to (Sanan et al 1994) this is about 10 nm. In Table S1 of SB we have used $\delta_{space} = 5x10^{-8}\ m$, see Sec. 3.1. In this case (15) yields 5. That means there are five levels of disturbing the multi-mutual inductance between nearby axons in CC. In Table 1 and Fig. 1b, the absolute value of $\varepsilon_{2,1}$ increases with D.

Regard the magnetic characteristics of inter-nerves that include capillaries with changing amount of oxygen in the brain. Hence, the magnetic susceptibility changes, as shown above. Recall in this paper we develop the theoretical idea that too high screening of EMMI in the brain might be the cause to AD. Hence, we use the parameter $\chi_{\text{int}nervs}$ for expressing the amount of shielding. It is plausible that each zone in the brain has its own range of normal limits of $\chi_{\text{int}nervs}$. For simplicity, we define "Biological MI shield" (BMIS), s_{bmi}, by

$$s_{bmi} \equiv \frac{4\pi}{\mu_0(1+\chi_{\text{int}nervs})} \qquad A^2/N \quad . \tag{16}$$

Recall $-9.249x10^{-6} \le \chi_{\text{int}nervs} \le -5.705x10^{-6}$. Thus, the normal lower and upper limits of BMIS are,

$$s_{bmi-\min} = \frac{4\pi}{\mu_0(1-5.705x10^{-6})}; \qquad s_{bmi-\max} = \frac{4\pi}{\mu_0(1-9.249x10^{-6})}. \tag{17}$$

Now, let us regard any zone in the brain, to be marked j. Its BMIS is s_{bmi-j}. The limits at *normal* conditions are $s_{bmi-j_{\min}}$ and $s_{bmi-j_{\max}}$. Recall there are five optional layers of βA between two nearby axons. Each level increases the BMIS. It is also clear that increasing the BMIS is equivalent to increasing the space between any two axons. Since there is no data for the susceptibility of βA, suppose for representing the idea, that each layer of βA increases that space by $1\delta_{space}$. Hence, the distance between axon-2 and layer *n* is

$$\delta_{space-n} = \delta_{space}(1+n). \tag{18}$$

Now we apply (18) on the programming that has led to Table 1. For representation, we list in Table 2 the decrease in % of the absolute value of $\varepsilon_{2,n}$ for $D = 0.1-1.0\,\mu m$. We see from Table 2 that the reductions in emf increases with increasing the number *n* of βA layers. In addition, as the axon diameter increases, the reduction decreases. This shows there might be axon systems that do not harm, due to specified addition of βA layers, while the other do.

Table 2. Reduction (%) of $\varepsilon_{2,n}$ due to increasing δ_{space} by the number *n* of βA layers, for various axon diameters *D*.

+n	1	2	3	4	5
D (micron)					
0.1	45	65	76	82	87
0.2	32	50	62	70	76
0.3	25	41	52	61	67
0.4	20	34	45	53	60
0.5	17	29	40	48	54
0.6	14	26	35	43	49
0.7	13	23	32	39	45
0.8	11	21	29	36	42
0.9	10	19	26	33	39
1.0	9	17	24	31	36

Suppose, for representation, that if there is a reduction of 65% in $\varepsilon_{2,n}$ of axon system, then those axons start being destroyed. From Table 2, the axons with $D = 0.1\,\mu m$ starts to be destroyed when are 2 layers of βA between all the many axons in that system. Destruction of axons might lead to creation of TA tangles. On the other hand, the axons with $D > 0.3\,\mu m$ not destroyed although 5 layers of βA exist between all the axons in those systems, i.e. no TA tangles appear. Now, for representing the idea, suppose that when TA tangles appear in between two axons, the BMIS increase in amount, which is equivalent to additional of $3\delta_{space}$ between the axons. From Table 2 we learn that in this case, the reduction of $\varepsilon_{2,n}$ in axon system with $D = 0.1\,\mu m$ is 87%. Suppose that when the reduction of $\varepsilon_{2,n}$ in axon system reach 85% there is no TC between the axons in this system. Hence, in those cases and

assumptions, the system with $D = 0.1\,\mu m$ stop the TC. On the other hand, the systems of axons with $D > 0.4\,\mu m$ might continue to have TC, even if TA tangles from systems with $D < 0.3\,\mu m$ inserted into the spaces between the axons. Hence, we see here an optional theoretical process for significant reduction in TC at certain axon-systems while at other axon-systems the TC not significantly infected. The axon-systems for whom TC significantly infected might show AD symptoms.

If the BMIS is between the normal limits, the electrical currents via the myelinated axons, which ends at the synapses, has the regular strengths. Those regular strengths include the weak negative streams due to the minus sign of the EMMI in (11). Now, if due to some reason $s_{bmi-j} > s_{bmi-j_{\max}}$, i.e. the BMIS is higher than the normal **upper** limit in zone j, the negative electric streams along axon-2 significantly reduced. That means the strength of the electric current **within** the axon is higher than the regular strengths. Hence, the rate of saltatory conduction increases beyond the upper normal limit. This might lead to damage of some nerves in zone j, and first βA might be created in zone j. This increases the BMIS even farther and more nerves in zone j are damage. At a critical value of BMIS, $s_{bmi-j_{critic}} > s_{bmi-j_{\max}}$, the axons in zone j start being **destroyed**, and first Tau tangles created. Now the BMIS in zone j is $s_{bmi-j} > s_{bmi-j_{critic}}$. The increasing BMIS increases the destruction of nerves in zone j. Hence, the process of increasing βA and Tau tangles continues. Thus, Alzheimer symptoms appear in zone j. At a certain time, the amount of βA and Tau tangles in zone j is so high that they start to diffuse to nearby zones. Hence, in those zones the BMIS increases and the process described for zone j occur in the nearby zones. In additions, amounts of βA and Tau tangles might transfer to far zones in the brain, and the process of nerves destruction in the brain might develop as a "snow ball". This is the beginning of the advanced stage of AD. Thus we saw a theoretical option for the creation of AD. The question is what causes to the **first** increasing of BMIS.

7. Optional reasons to creation of too high BMIS

Since we saw in Sec. 6 the optional dangerous process due to too high screening of EMMI, we try to find out the catalysator to that process. There might be many reasons to the creation of too high BMIS. Each of the long list of optional reasons to AD might cause to creation of too high BMIS: genetic, illness, viruses, degradation of immune system, injury, etc. This includes the recent research (Kumar et al 2016) that shows βA plaques play positive role in fighting off bacteria and fungus in mice, worms and cells, by surrounding them and caging them in. Recall that clumps of βA plaques considered for long time as the hallmark of AD. Such clumps of βA plaques found linked onto brain nerves and damage them. Hence, (Kumar et al 2016) suggest the option the reason to AD are bacteria and fungus in brain, while the fight of the brain against those bacteria and fungus creates the clumps of βA . We saw above that clumps of βA enlarge the BMIS and screens the mutual inductance between nerves.

Statistics shows most of the AD events appear after 65 age. Hence, due to my understanding of the crucial importance of EMMI in all brain activities, I suspect the main reasons to creation of high BMIS is a **drastic** change in physical and/or mental behavior, when people **retire** at, say, 62-65, following many years of doing specific physical and/or mental actions. At youth the body and mind build themselves according to the occasional changes. During those years, the limits of normal s_{bmi} at the various zones in the brain are created and adapt themselves to the new conditions. However, if in one or more zones the BMIS is much higher than the upper limit of s_{bmi}, there might begin a series of actions in the nerve

system that eventually yield AD symptoms. As hypothetical example let us regard an athletic person. From youth, he develops mainly the zones in the brain that controls the specific muscles for his specified skill. Suppose in addition that this person does not paint. Hence, the "athletic zones" (AZ) are more active than the "painting zones" (PZ). Hence, the EM mutual inductance between nerves is higher in AZ then in PZ. That means the maximal value of s_{bmi} in AZ is lower than in PZ, i.e. $s_{bmi-AZ_{\max}} < s_{bmi-PZ_{\max}}$. Now suppose at age 65 this athletic person retires and decides to leave the sport and devote his rest life to painting. He enjoys the new occupation of painting and continues to paint for years. The activity of the nerves in PZ increases. But, the activity in AZ dramatically decreases. After 1-2 years the nerves in AZ start degeneration. Hence, the first β **-Amyloid plaques** appear in AZ. This increases gradually s_{bmi} in AZ till $s_{bmi-AZ} > s_{bmi-AZ_{\max}}$. I assume that at this stage begins the destruction of nerves in AZ. Hence, the first **Tau tangles** appear in AZ. Thus, s_{bmi-AZ} increases even more and the way to Alzheimer symptom in AZ is open, as explained above. At age 67 that person might enjoys the painting but suffer from first Alzheimer symptoms. In this hypothetical example, we saw an optional way for increasing s_{bmi} at specific zones, the "athletic zones". This scenario might be for any other kind of occupation: academic, teaching, playing, singing, house builder, etc. For those cases one may replace the word "athletic" by "academic", "teaching", etc.

8. Suggestion for optional detecting AD status

We saw the importance of knowing the BMIS at the various brain zones to prevent AD and to monitor its status. We suggest here the option of using regular EEG tests, say every 2-3 years from age 50, and comparing the data. The EEG not invasive. It may show the normal TC and be compared to abnormal TC. Deep research might map the normal limits of s_{bmi}, at various brain zones, for the healthy person at age 50, i.e. before the commencement of first βA plaques. After several years, some persons might have, at certain zones, $s_{bmi} > s_{bmi-upper}$. In this case, the EEG might show lower strength or unusual frequencies at those zones. Later, the EEG might show increasing s_{bmi}, in accordance with the development of AD. Those data, in addition to data from other means, might help to choose the best strategy to defeat AD.

9. **Research for proving EEMI between multi myelinated axons** and its screening

I am not experimental researcher, but I may point out at three optional methods for proving the notion of EMMI between multi myelinated axons and its screening: a) growing nerves with myelinated axons in petri dishes, so they simulate the situation in the splenium of adult human; measure the EMMI over the central axon; add some βA plaques and measure the difference. Reduction in EMMI's strength points out at screening. b) using EEG on healthy animal's brain; add some βA plaques to their brain and measure the reduction in EEG strength. c) measure reduction in strength of EEG on human brains that start showing AD signals, as function of βA and Tau amounts measured by CT, MRI, etc. Experimental researchers might suggest additional methods.

10. Suggestion to measure the shielding, s_{bmi}, in the brains of many million people during Sun Eruptions

This section discusses sun eruptions and shielding in the human brain. Recently there is increase interest in the connection between sun eruptions and human diseases. The influence might occur during intense geomagnetic storm, which is a worldwide disturbance of the Earth's magnetic field, associated with solar activity. The geomagnetic storms arrive to Earth after 1-3 days of Coronal spirals ejection in sun atmosphere. Sun eruptions occur in cycle of about 11 years and might lapse 2-3 years during which might be very strong Coronal spirals eruptions. Let us cite some important facts.

From "Space Weather" of NASA: " The most serious effects on human activity occur during major **geomagnetic storms**. It is now understood that the major geomagnetic storms are induced by coronal mass ejections (CMEs). Coronal mass ejections are usually associated with flares, but sometimes no flare is observed when they occur. Like flares, CMEs are more frequent during the active phase of the Sun's approximately 11 year cycle. The last maximum in solar activity, the maximum of the current solar cycle, was in April, 2014**".**

Papathanasopoulos et-al 2016 shows a correlation between sun eruptions and multiple sclerosis (MS): " The rate of MS patient admittance due to acute relapses was found to be associated with the solar and geomagnetic events. There was a “primary” peak in MS admittance rates shortly after intense geomagnetic storms followed by a “secondary” peak 7–8 months later."

On the other hand, Staša Milojević 2016 shows **no correlation** between sun eruptions and primary headaches and migraines. He used millions of Twitter massages referring to headaches and migraine between November 2012 and January 2016: " The most intense geomagnetic storm of the current solar cycle (Cycle 24) occurred on June 22, 2015, with the maximum value of global (planetary) 3-hr index *ap* index) of 230. The index measures the disturbance of the Earth’s magnetic field near its surface. "

I do not find a work regarding sun eruptions and Alzheimer disease (AD). However, if my idea of shielding in between brain axons, is true, then one might expect that increasing in local magnetic strength on Earth, due to a major geomagnetic storm, might overcome some levels of brain shielding. This is analogues to the existence of a shielding liquid between two transparent glasses, e.g. milk in a glass cup. Week light may not penetrate through the glasses. However, strong light may penetrate and yields a weaker light at the other side. Thus, in some patients with Early and Moderate AD stages, one might expect temporally improvement in their memory, during the period of major geomagnetic storm, and/or short time after. In addition, in people that are only at the start of increasing shielding above the upper normal limit, but long time before the appearance of first known markers of Early AD, a memory test, during major geomagnetic storm, might show a small temporal improvement, relative to not being exposed to increasing local magnetic fields due to geomagnetic storm. Such memory tests might be markers of the s_{bmi} levels in the brains of many million people over the world, at a short period. In Table 3 given **hypothetical** example of a matrix memory levels, as function of the **magnetic energy amount (MEA)**, i.e. increasing local magnetic intensity multiplied by exposer time, and of the shielding levels s_{bmi}.

Let us use the hypothetical Table 3 to explain this feature. Let **person-1** be exposed to MEA **0** and suppose his memory, at that moment, is at level **4.** According to Table 3, his s_{bmi} level is N+, i.e. just above the upper limit of the normal s_{bmi} range. If person-2 stands near person-1 for the same period, and his memory level is 3, that hints his s_{bmi} level is A1, i.e. at **Early** AD stage. If person-3 stands near person-1 for the same period, and his memory level is 2, that hints his s_{bmi} level is A2, i.e. at **Moderate** AD stage, and so on regarding the same row MEA 0. If a person exposed to MEA **5** and his memory level is **3.5** then, according to the hypothetical Table 3, his s_{bmi} level is A3, i.e. at **Advanced** AD stage.

Notice that according to that Hypothetical Table 3, a person with s_{bmi} level A4, i.e. at **Very advanced** AD stage, which exposed to MEA **6**, its memory level may have a small increase to **0.6**.

Table 3 – Hypothetical example of a matrix memory levels, as function of the **Magnetic Energy Amount (MEA),** i.e. the increase in magnetic energy intensity multiplied by the exposer time**, and of the shielding levels s_{bmi}.**

s_{bmi}: ---------- MEA	N+	A1 (Eearly AD stage)	A2 (Moderate AD stage)	A3 (Advanced AD stage)	A4 (very advanced AD)
0	4	3	2	1	0
1	5	4	3	1.5	0.1
2	6	5	4	2.0	0.2
3	7	6	5	2.5	0.3
4	8	7	6	3.0	0.4
5	9	8	7	3.5	0.5
6	10	9	8	4.0	0.6

This table is **hypothetical**. Experiments are expected to yield a realistic table. Upon giving the data of memory level and MEA, one may use a realistic table to find out the s_{bmi} level.

I expect improvement in memory due to increase in MEA. However, there might be cases, mainly in moderate and advanced AD stages, where the influence of increasing MEA might yield opposite results, i.e. reduction in memory level, pending on various causes. This should be checked by experimental researchers using technological tools.

There is also an option to perform other mental tests, to measure s_{bmi} levels during major sun eruptions, not only memory tests. Those are also subject to experimental research before applying on many people.

At the bottom line, the influence of sun eruptions on brains with various levels of s_{bmi}, is now at the theoretical ideas level. However, if some of those ideas approved, this might be a new tool to help many million people to get an alarm and to start implying active actions to prevent AD. The organization that supply geomagnetic storm events and predict their occurrence and their strength is **NOAA Space Weather Prediction Center**.

Note: Since the ideas in this article are theoretical, yet without laboratory research, one should not regard these ideas as clinical suggestions.

Conclusion

In this theoretical work sown that for a group of many parallel myelinated axons, in the human corpus callosum, the EM **mutual multi-inductance** might have **significant influence** on the electrical conduction of each axon in the group. Theoretically shown that the mutual inductance may lead to transverse communications (TC) between many axons, in addition to the familiar longitudinal communications (LC) via the synapses. Existence of too much beta-Amyloid (βA) plaques in-between the axons increases the EM shielding between the axons. This might reduce TC and LC, up to a level where axons destructed. This destruction might lead to creation of Tau tangles (TA) and βA, which might be distributed among the healthy axons, and increase the EM shielding in between those axons. Hence, the process of increasing shielding, reducing TC and LC, and destruction of axons might be developed as a "snow ball" and leads to the symptoms of Alzheimer disease (AD). We point out at the option that the trigger to the first occurring of too much βA is the drastic change in physical and/or mental behavior, when people **retire** following many years of doing specific physical and/or mental actions. Suggested using EEG for monitoring EMMI shielding, and thus, AD status. In addition, suggested research methods for proving EEMI between multi myelinated axons and its screening. Also suggested to measure the memory of many million people during a major geomagnetic storm on Earth due to sun eruption, in order to find out the level of shielding in many million people and getting alarm, years before the common signs of AD appears, and start active actions to prevent AD.

Note: Since the ideas in this article are theoretical, yet without laboratory research, one should not regard these ideas as clinical suggestions.

References

Abiotiz F et al 1992, Morphometry of the Sylvian fissure and the corpus callosum, with emphasis on sex differences, Brain **115**: 1521-1541.

Aebischer HA and Aebischer B 2014, Improved formulae for the inductance of straight wires, Advanced Electromagnetics **3**(1).

Bakiri Y et-al 2011, Morphological and electrical properties of oligodendrocytes in the white matter of the corpus callosum and cerebellum, *J Physiol* 589.3 : 559–573.

Bishop KM and Wahlsten D 1997, Sex differences in the human corpus callosum: myth or reality?, Neuroscience and Biobehavioral Reviews **21**(5): 581-601.

Caminiti R et al 2009, Evolution amplified processing with temporally dispersed slow neuronal connectivity in primates, PNAS **106** (46): 19551–19556.

Chen TY et-al 2015, Far-Infrared therapy promotes nerve repair following end-to-end neurorrhaphy in rat models of Sciatic nerve injury, Hindawi Publishing Corporation, Evidence-Based Complementary and Alternative Medicine, Volume 2015.

Collin G et al 2016, Brain network analysis reveals affected connectome structure in bipolar I disorder, Human Brain Mapping **37**:122–134.

Goodman G and Bercovich D 2013, Electromagnetic induction between axons and their schwann cell myelin-protein sheaths, Journal of Integrative Neuroscience, Vol. 12, No. 4 (2013) 475–489.

Grubb MS and Burrone J 2010**,** Activity-dependent relocation of the axon initial segment fine-tunes neuronal excitability, Nature **465**, 24 June 2010.

Hodgkin AL and Huxley AF 1952, A quantitative description of membrane current and its application to conduction and excitation in nerve, J. Physiol. **117,** 500–544.

Hursh JB 1939, Conduction velocity and diameter of nerve fibers, Am J Physiol **127**: 131–139.

Kumar DKV et al 2016, Amyloid-β peptide protects against microbial infection in mouse and worm models of Alzheimer's disease, www.ScienceTranslationalMedicine.org**, 25 May 2016,** 8(340): 340ra72.

Liewald D et al 2014, Distribution of axon diameters in cortical white matter: an electron-microscopic study on three human brains and a macaque, Biol Cybern **108**: 541–557.

Opatowski I 1950, The velocity of conduction in nerve fiber and its electric characteristics, Bulletin of Mathematical Biophysics **12** (4), 277-302.

Papathanasopoulos P. et al 2016, The possible effects of the solar and geomagnetic activity on multiple sclerosis, Clinical Neurology and Neurosurgery 146 (2016) 82–89.

Plascencia-Villa G et al 2016, High-resolution analytical imaging and electron holography of magnetite particles in amyloid cores of Alzheimer's disease, Scientific Reports **6:** 24873.

Rotem A and Moses E 2008, Magnetic stimulation of one-dimensional neuronal cultures, Biophysical Journal **94**: 5065–5078.

Roth BJ and Wiksow JP 1985, The magnetic field of a single axon, Biophys. J. **48,** 93-109.

Sanan DA et al 1994, Apolipoprotein E associates with β Amyloid peptide of Alzheimer's disease to form novel monofibrils, J. Clin. Invest **94**: 860-869.

Schenck JF 2000, Safety of strong, static magnetic fields, Journal of Magnetic Resonance Imaging **12**: 2–19.

Scott AC 1971, Effect of the series inductance of a nerve axon upon its conduction velocity, Mathematical Biosciences **11**, 277-290.

Space weather of NASA, https://hesperia.gsfc.nasa.gov/sftheory/spaceweather.htm

Staša Milojević 2016, Revisiting the connection between Solar eruptions and primary headaches and migraines using Twitter, Sci Rep. 2016; 6: 39769. Published online 2016 Dec 23.

Wang H et al 2018, Inductance in neural systems, bioRxiv preprint first posted online Jun. 13, 2018; doi: http://dx.doi.org/10.1101/343905.

Wijesinghe RS 2010, Magnetic measurements of peripheral nerve function using a neuromagnetic current probe, Experimental Biology and Medicine **235**: 159–169.

Zborowski M et al 2003, Red blood cell magnetophoresis, Biophysical Journal **84**: 2638–2645.

Supplementary

Supplementary A. A model of axons at many concentrating circles

In this supplementary A (SA) we develop a model of axons at many concentrating circles, while at the center is an axon regarding to which all the axons have EM mutual inductance. In Fig. 4 of (Liewald et al 2014) shown the way they measured the inner diameter of myelinated axons. Most of the axons have *elliptical* shape. The measured diameter, D_{inner}, is the short axis of the ellipse. Let us mark half of that diameter by a_{inner}, i.e.

$$a_{inner} = \frac{D_{inner}}{2} \ . \tag{S1}$$

The long half axis of such ellipse marked by b_{inner}. Let us define the ratio parameter

$$k_{inner} = \frac{b_{inner}}{a_{inner}} . \tag{S2}$$

Since the magnetic flux in (2) obtained for area, we may replace the inner ellipse axon by inner *circular* axon with the same area, i.e. $A_{inner-circle} = A_{inner-ellipse}$. Hence, the radius of this circle is

$$R_{inner} = \frac{D_{inner}}{2}\sqrt{k_{inner}} \ . \tag{S3}$$

We use this inner radius for computing the EMMI between *two* axons in (5).

For treating multiple axons, we need the radius of the *myelinated* axon. Let the thickness of myelin sheath be W_{axon} and let $W_{axon} = D_{inner}/3$. Assume the same myelin width around the ellipse. Thus, the external axes of the myelinated ellipse axon are $a_{myelin-axon} = a_{inner} + W_{axon}$ and $b_{myelin-axon} = b_{inner} + W_{axon}$. Insert here (S2) yields

$$b_{myelin-axon} = k_{inner}a_{inner} + W_{axon} . \tag{S4}$$

The area of the myelinated ellipse axon is $A_{myelin-ellips} = \pi a_{myelin-axon}b_{myelin-axon}$. Hence,

$$A_{myelin-ellips} = \pi (a_{inner} + W_{axon})(k_{inner}a_{inner} + W_{axon}) . \tag{S5}$$

Since the magnetic flux in (2) obtains for area, we may replace the myelinated ellipse axon by a myelinated circular axon with the same area, i.e.

$$A_{myelin-circle} = A_{myelin-ellipse} \ . \tag{S6}$$

Now $A_{myelin-circle} = \pi R^2_{myelin-axon}$, where $R_{myelin-axon}$ is the radius of a circular myelinated axon. Hence, from (S5), (S6) and (S1) obtained

$$R_{myelin-axon} = \frac{1}{2}\sqrt{(D_{inner} + 2W_{axon})(k_{inner}D_{inner} + 2W_{axon})} . \tag{S7}$$

For the case $W_{axon} = D_{inner}/3$ and $k_{inner} = 1.5$, we obtain from (S7)

$$R_{myelin-axon} = 0.95D_{inner} , \tag{S8}$$

i.e. the radius of the circular myelinated axon is about the short axis of the elliptical axon.

As shown in Fig. 7 of (Liewald et al 2014), the axons in a small section of the corpus callosum (CC) of a monkey Macaque has various diameters. This is also true for human CC. Thus, if one wishes to compute the mutual inductance between a specific axon and between all the other axons, one should regard the various diameters and distances of the axons in that section. However, as in many cases in electrodynamics, since the conduction velocity increases approximately linearly with axon diameter (Hursh 1939), one may use an equivalent method: Regard a specific section with myelinated axons of various internal diameters. Let the *mean* internal diameter of the axons be D_{mean} and let the section area be $A_{\text{section.}}$. This is the cut surface that includes the axons, each of which is a cut surface of a myelinated axon, as in the case of the splenium. From Fig. 7 of (Liewald et al 2014) we see there is a about a constant space between the myelinated axons, regardless the axon diameter. This space is required for the saltatory conduction mechanism, i.e. to supply the Na^+ from the surrounding of the Ranvier node. Let us mark this constant distance by $2\delta_{space}$ and regard many equal *tiny* circles with radius

$$R_{tiny} \equiv R_{myein-axon} + \delta_{space} \,. \tag{S9}$$

Regard axon-2 at that system origin, having radius R_{tiny}. Arrange the tiny circles around axon-2 in layers, without space between the layers, as follows. The first layer has 6 tiny circles. The second layer 12, and so on, increasing by 6 from one layer to the next. The radius enclosed by layer *n* is

$$R_n = (1+2n)R_{tiny} \,. \tag{S10}$$

Hence, the area enclosed by layer *n* is

$$A_{layer-n} = \pi(1+2n)^2 R_{tiny}^2 \,. \tag{S11}$$

The number of tiny circles *up* to layer n is

$$N_{circes-n} = 1+3n+3n^2 \,. \tag{S12}$$

Hence, the total area of those $N_{circles-n}$ tiny circles is

$$A_{N_{circles-n}} = \pi R_{tiny}^2 (1+3n+3n^2) \,. \tag{S13}$$

Divide (S11) by (S13) yields

$$\frac{A_{layer-n}}{A_{N_{circles-n}}} = \frac{1+4n+4n^2}{1+3n+3n^2} \,. \tag{S14}$$

For $n > 1000$ this ratio yields 1.333. Hence we define

$$A_{layer-n-reduced} \equiv A_{layer-n}/1.333 \ . \quad \text{(S15)}$$

For the maximal value of *n*, $n_{\max}$,

$$A_{layer-n_{\max}-reduced} = A_{layer-n_{\max}}/1.333 \ . \quad \text{(S16)}$$

Now, $A_{layer-n_{\max}} = A_{section}$. Hence,

$$A_{section-reduced} = A_{section}/1.333. \quad \text{(S17)}$$

Now we can find out the number of tiny circles in the reduced area:

$$N_{tiny} = \frac{A_{section-reduced}}{\pi R_{tiny}^2}. \quad \text{(S18)}$$

The density is

$$\rho_{tiny} = \frac{N_{tiny}}{A_{section}}. \quad \text{(S19)}$$

Hence (S12) for $n_{\max}$ is

$$N_{tiny} = 1 + 3n_{\max} + 3n_{\max}^2 . \quad \text{(S20)}$$

The solution of this for $N_{tiny} >> 1$ is

$$n_{\max} = 0.577\sqrt{N_{tiny}} . \quad \text{(S21)}$$

Insert this into (S10) yields

$$R_{n_{\max}} = \left(1 + 1.155\sqrt{N_{tiny}}\right)R_{tiny}. \quad \text{(S22)}$$

Notice, for EMMI computation we need R_{inner} of (S3), where the electric current flows, not R_{tiny}.

Supplementary B. Table S1.

Computations of MI-N at Splenium area for variuos optional mean axon diameters												
Constant Input data												
Splenium area	8.50E-05	m^2										
W/D	1/3											
k_{inner}	1.5											
δ_{space}	5.00E-08	m										
l_{axon}	1.504E-01	m										
$\mu_{nerv-nerves}$	1.26E-06	(mu-0)										
Changing input data												
D-axon	**m**		**1.00E-07**	**2.00E-07**	**3.00E-07**	**4.00E-07**	**5.00E-07**	**6.00E-07**	**7.00E-07**	**8.00E-07**	9.00E-07	1.00E-06
dI/dt	A/s		1.2E-08	2.4E-08	3.6E-08	4.8E-08	6.00E-08	7.20E-08	8.40E-08	9.60E-08	0.000000108	0.00000012
Output												
W	m		3.33E-08	6.67E-08	1.00E-07	1.33E-07	1.67E-07	2.00E-07	2.33E-07	2.67E-07	0.0000003	3.33333E-07
R-myelin	m		9.50E-08	1.90E-07	2.85E-07	3.80E-07	4.75E-07	5.70E-07	6.65E-07	7.60E-07	8.55132E-07	9.50146E-07
R-tiny	m		1.45E-07	2.40E-07	3.35E-07	4.30E-07	5.25E-07	6.20E-07	7.15E-07	8.10E-07	9.05132E-07	1.00015E-06
N-tiny			9.65E+08	3.52E+08	1.81E+08	1.10E+08	7.36E+07	5.28E+07	3.97E+07	3.09E+07	2.48E+07	2.03E+07
ρ_{inn}	1/m^2		1.14E+13	4.14E+12	2.13E+12	1.29E+12	8.66E+11	6.21E+11	4.67E+11	3.64E+11	2.91399E+11	2.38663E+11
n-max			17924	10829	7758	6044	4950	4192	3635	3208	2872	2599
M2,1 (mu-0)	(mu-0)		3.7439E-07	3.59E-07	3.49E-07	3.42E-07	3.36E-07	3.31E-07	3.26E-07	3.23E-07	3.19308E-07	3.16305E-07
M2,1	(Nm/A^2)		4.7047E-13	4.51E-13	4.39E-13	4.29E-13	4.22E-13	4.16E-13	4.10E-13	4.05E-13	4.01254E-13	3.97481E-13
e-2,1	V		-5.65E-21	-1.08E-20	-1.58E-20	-2.06E-20	-2.53E-20	-2.99E-20	-3.45E-20	-3.89E-20	-4.33354E-20	-4.76977E-20
e-2,1	mV		-5.646E-18	-1.08E-17	-1.58E-17	-2.06E-17	-2.53E-17	-2.99E-17	-3.45E-17	-3.89E-17	-4.33354E-17	-4.76977E-17
e-2,1	(10^17 mV)		-0.56	-1.08	-1.58	-2.06	-2.53	-2.99	-3.45	-3.89	-4.33	-4.77
sum ([]*6n)			5.19E+08	1.89E+08	9.73E+07	5.90E+07	3.96E+07	2.84E+07	2.14E+07	1.66E+07	1.33E+07	1.09E+07
M2,N (mu-0)	mu-0		103.82	37.90	19.45	11.81	7.92	5.68	4.27	3.33	2.67	2.18
M2, N	(Nm/A^2)		0.00013047	4.76E-05	2.44E-05	1.48E-05	9.95E-06	7.14E-06	5.37E-06	4.18E-06	3.35007E-06	2.74356E-06
e-2,N (V)	V		-1.51E-03	-4.03E-04	-1.59E-04	-7.81E-05	-4.39E-05	-2.71E-05	-1.79E-05	-1.24E-05	-8.96E-06	-6.68E-06
e-2,N (mV)	mV		-1.511	-0.403	-0.159	-0.078	-0.0439	-0.0271	-0.0179	-0.0124	-0.0090	-0.00668

The meanings of short terms in this article

A – cat surface of conductor.

$A_{section}$ - section area.

$A_{splenium}$ - splenium area.

AD - Alzheimer disease.

B - magnetic field.

CC - corpus callosum.

d – distance.

D_{inner} - measured diameter of axon.

D_{mean} - *mean* internal diameter of the axons.

$d_{two\ axons}$ - the distance between the two axons, which includes the myelin thickness and the space between the myelinated axons (see Eq. 5).

$D_{splenium}$ - internal diameters in a small area of the splenium.

EM - Electromagnetic.

EMMI - EM mutual-inductance.

I - electrical current.

dI_{axon}/dt - the gradient of current with time (see Eq. 7).

l - length.

l_{axon} - axon length.

M - mutual inductance.

M_{21} - mutual inductance in conductor-2 due to current in conductor-1.

$M_{21,\,axons}$- the EMMI over axon-2 due to alternate current in axon-1 (see Eq. 5).

$M_{21-destruct}$- the destructive level (see Eq. 13).

$M_{21-prevent}$- the preventing level (see Eq. 13).

MEA - Magnetic Energy Amount (see Table 3 in Ch. 10).

$n_{\max}$ - the maximal number of layers.

N_{tiny} - the number of tiny circles.

R_{inner}- the circular inner radius for a circle of the same area as that of the inner ellipse of the bar-axon, without myelin.

$R_{myelin-axon}$ - the radius of a circular myelinated axon.

R_{tiny} - the radius of a *tiny* circle about the axon.

s_{bmi} - biological MI shield (see Eq. 16).TC - transverse communications.

LC - longitudinal communications.

$W_{\beta A}$ - the width of a single ribbon of βA.

Z – impedance.

βA - β -Amyloid.

ε - electromotive force (emf).

$2\delta_{space}$ - the distance between the myelin surfaces of two nearby myelinated axons.

ϕ - magnetic flux.

ϕ_{21} - the magnetic flux within conductor-2, due to the current in conductor-1.

μ - magnetic permeability of the medium surrounding the conductor.

μ_0 - magnetic permeability in free space.

$\mu_{inter-nerves}$ - the magnetic permeability of the matter between those two axons (see Eq. 5).

χ - the susceptibility defined by the connection $\mu = \mu_0(1+\chi)$.